Journal of the Korean Physical Society, Vol. 71, No. 11, December 2017, pp. 780∼784

Angular Distributions of Bremsstrahlung Photons from ECR Plasma

M. J. Kumwenda, J. K. Ahn,* J. W. Lee and I. J. Lugendo
Department of Physics, Korea University, Seoul 02841, Korea

S. J. Kim, J. Y. Park and M. S. Won
Busan Center, Korea Basic Science Institute, Busan 46241, Korea

(Received 21 June 2017, in final form 12 September 2017)

High-energy bremsstrahlung photon emission beyond a critical energy from electron cyclotron resonance (ECR) heating has long attracted much attention, and its nature has yet been unsolved. We have measured bremsstrahlung photons from the 28-GHz ECR ion source at Busan Center of Korean Basic Science Institute. The gamma-ray detection system consists of three NaI(Tl) scintillation detectors placed 62 cm radially from the beam axis and a NaI(Tl) scintillation detector at the extraction port for monitoring the photon intensity along the beam axis. Bremsstrahlung photon energy spectra were measured at nine azimuthal angles at the RF power of 1 kW. Azimuthal angular distributions of bremsstrahlung photons were found to be in coincidence with the structure the ECR ion source and the shape of ECR plasma.

PACS numbers: 29.25.Ni, 29.30.Kv, 52.25.Os, 52.50.Sw, 52.70.La
Keywords: ECR ion source, Bremsstrahlung photons, NaI(TI) detector, Microwave power
DOI: 10.3938/jkps.71.780

I. INTRODUCTION

Electron cyclotron resonance (ECR) ion sources are used to produce intense, highly multiple-charged ions [1, 2]. In the ECR ion source electrons are heated resonantly by microwaves to provide ionization of neutral gases [3, 4]. During the bombardment of electrons, the ions or atoms are ionized, leading to charges up to the maximum charge with all electrons stripped off. A highly charged ion generates bremsstrahlung photons emission when it is decelerated or stops in materials [5,6].

In the ECR ion source, two processes in the plasma lead to the emission of bremsstrahlung photons. In the first process bremsstrahlung radiation is generated by electron-ion or electron-electron collisions within the plasma volume. The second process happens when unconfined electrons strike the chamber wall and lose their energy through interaction with the wall material [7–9]. The bremsstrahlung photon produced by these two processes can penetrate through the plasma chamber, and consequently, add substantial heat load to the cryostat when they are absorbed in the cold mass [10].

Measurements of bremsstrahlung photons from ECR ion sources have been performed since late 1960s [11]. However, most previous experiments measured the bremsstrahlung photons only in one direction, either radially or axially using one or two detectors under different conditions. Nevertheless, the bremsstrahlung radiations emitted from the ECR plasma is expected to be anisotropic due to various effects [12]. It is very crucial to measure the angular distributions of bremsstrahlung photons on the extraction side of the ECR ion source.

This paper presents the first measurement results of azimuthal angular distributions of bremsstrahlung photons from the 28-GHz ECR ion source in nine azimuthal angles.

II. EXPERIMENT

The experiment was carried out to measure bremsstrahlung photons from the 28-GHz superconducting ECR ion source of the compact linear accelerator facility at Busan Center of Korea Basic Science Institute (KSBI) [13]. The KBSI accelerator was developed to produce high-intensity fast neutrons for high-resolution radiography.

The superconducting magnet system consists of three mirror solenoid coils and a hexapole magnet. The axial magnetic field strengths reach 3.6 T at the beam injection section and 2.2 T at the extraction section, respectively. A radial magnetic field of 2.1 T is produced at the plasma chamber wall. The cylindrical plasma chamber is 500 mm long and 150 mm in diameter, respectively. The chamber is made of a stainless steel (SUS316L), and the chamber volume is kept at a ultra-high vacuum of 10^{-8}

*E-mail: ahnjk@korea.ac.kr; Fax: +82-2-3290-3093

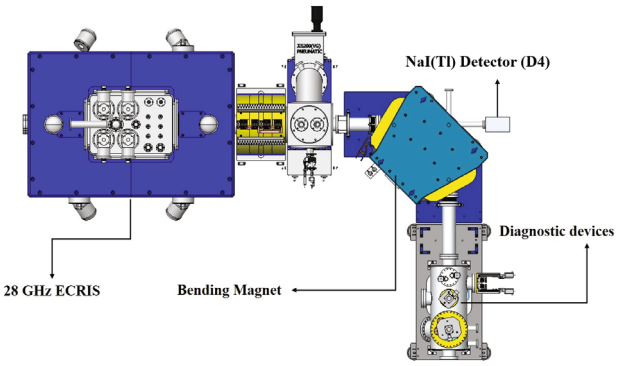

Fig. 1. (Color online) Schematic view of the low-energy accelerator facility at Busan Center of KBSI. An NaI(Tl) detector is placed at the view port of a bending magnet.

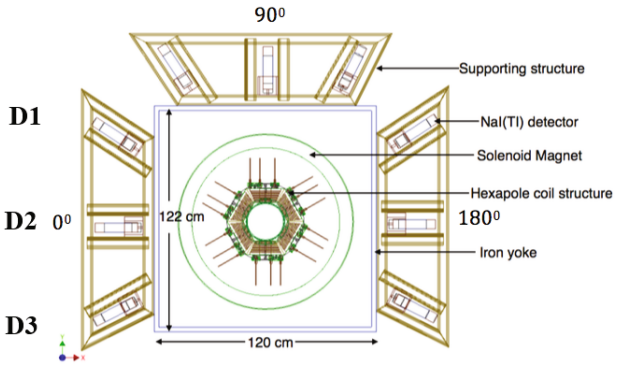

Fig. 2. (Color online) Schematic view of three round type NaI(TI) detectors extraction side (radial).

Torr. The inner face of the hexapole coil is 207 mm from the beam axis, and the coil thickness is 90 mm. The periodic structure of the hexapole coils could block bremsstrahlung photons. The inner face of the 102-mm thick solenoid coil is placed at a distance of 416 mm from the beam axis. The 50-mm thick iron shielding structure is 1200 mm wide, 1220 mm high and 1700 mm long.

Oxygen ion beam was extracted at the beam currents of 300 μA for O^{3+} and 30 μA for O^{5+}. The extraction voltage was 10 kV and the RF power was 1 kW. The bremsstrahlung photon measurement was performed using four identical NaI(Tl) detectors (ORTEC 905-3 series). The NaI(Tl) crystal is 2 inch in diameter and 2 inch in length, which is optically coupled to a photomultiplier tube. The crystal is encapsulated in a light-tight aluminum case. The detectors are labeled as D1, D2, D3, and D4, respectively, which were operated at +1300 V. The three detectors (D1, D2, and D3) were mounted on the support structure for measurements at azimuthal angles, as shown in Fig. 2, while the D4 detector was mounted at the view port for monitoring the intensity of ECR plasma.

We first measured the angular distribution of bremsstrahlung photons from the 28-GHz ECR ion source at 1 kW. The photon energy was measured at

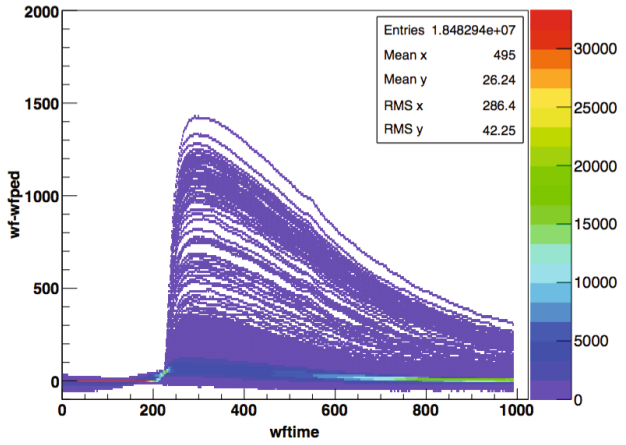

Fig. 3. (Color online) Superimposed NaI(Tl) detector signals digitized using a 500-MHz flash ADC.

nine angles in a 30° interval. The detectors were placed at the three sides (top, left and right) of the iron shielding structure. The three detectors were first mounted on a single support structure, and changed the positions, to cover the angular region. For a systematic study among the three detectors, the three detectors were exchanged at the same angular position. The detector face was approximately 20 mm from the iron shielding structure.

Each NaI(Tl) detector was placed in a Pb collimator of $100 \times 100 \times 100$ mm^3 with a 5-mm hole. The Pb collimator covered a full dimension of the NaI(Tl) crystal. The detector signal was fed to a 500-Hz flash ADC and recorded in a two-fold coincidence with a reference signal from the detector D4 placed at the view port. The 4-channel flash ADC module (Notice Co.) recorded a full pulse information from four NaI(Tl) detectors in every 32 μs. Typical pulse shapes are superimposed in Fig. 3. The ring-buffer data were then fed to a PC. Due to a huge data size, the measurement was performed in every three minutes. Background photon energy spectrum was taken for 15 hours, as shown in Fig. 4. A bump near 1.46 MeV corresponds to γ-rays from ^{40}K, and a peak near 2.6-MeV is associated with ^{206}Tl. The background spectrum was normalized with the data-taking time and subtracted from raw spectra for bremsstrahlung photon measurement.

During the detector replacements the calibration data were taken using characteristic γ rays from radioactive sources, ^{137}Cs (662 keV) and ^{60}Co (1173 keV and 1332 keV) [14]. Three calibration data points were fitted with a linear straight line using a least-squared χ^2 fit.

Due to a complicated structure of the ECR ion source, the material budget differs largely depending on the azimuthal angles. The rectangular cross section of the ion shielding structure and the race-track hexapole coil structure give a large non-uniformity in the material budget. A Geant4 simulation was performed to take the geometric acceptance and also the energy-dependent detection efficiency into account. The energy range is grouped

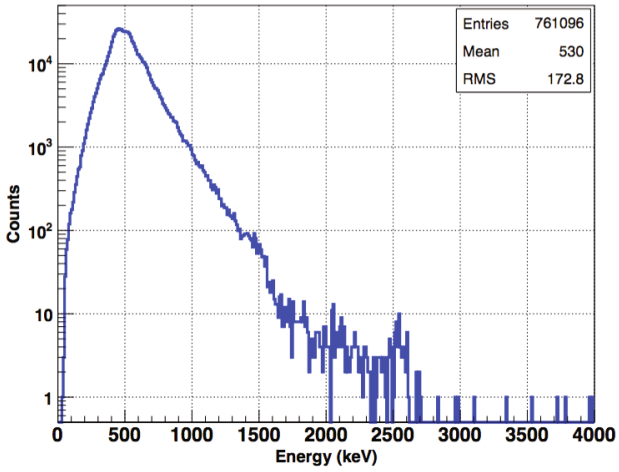

Fig. 4. (Color online) Background photon energy spectrum taken for 15 hours.

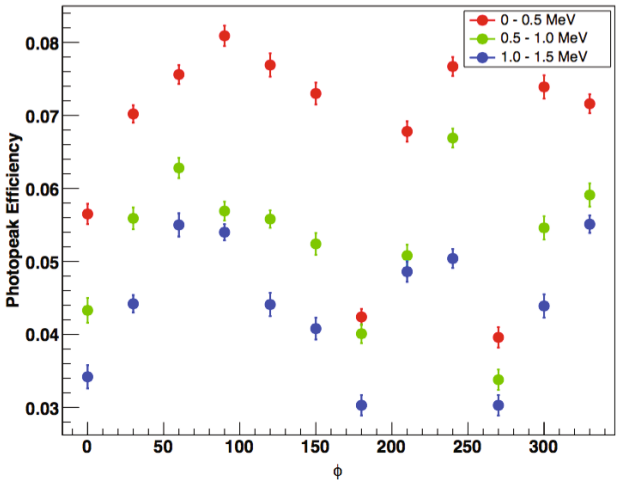

Fig. 5. (Color online) Full photo-peak efficiencies were obtained from a Geant4 simulation in three energy regions.

into three energy regions: low-energy ($E_\gamma < 0.5$ MeV), mid-energy ($0.5 < E_\gamma < 1.0$ MeV), and high-energy ($E_\gamma > 1.0$ MeV). Figure 5 represents the full photo-peak efficiencies regarding the azimuthal angle and the energy region, based on a Geant4 simulation. The simulation results were obtained for a point source emitting continuous energy photons in each energy region. The detection efficiencies are expected to oscillate with a periodic structure of the hexapole coils. However, the low-energy efficiencies lead the other two energy efficiencies by 30°, while the mid-energy and high-energy data are in phase.

For the low-energy region the efficiency peaks at 90° and 270°. The detector plane came across the rounding corners of the hexapole coils. Therefore, only the gaps between the adjacent hexapole coils could account for the anisotropic distributions at every 60° from 0°. In the mid-energy and high-energy regions, the full photo-peak efficiencies reach the maxima at 60°, 240° and 330°. The additional support structure of the ECR ion source

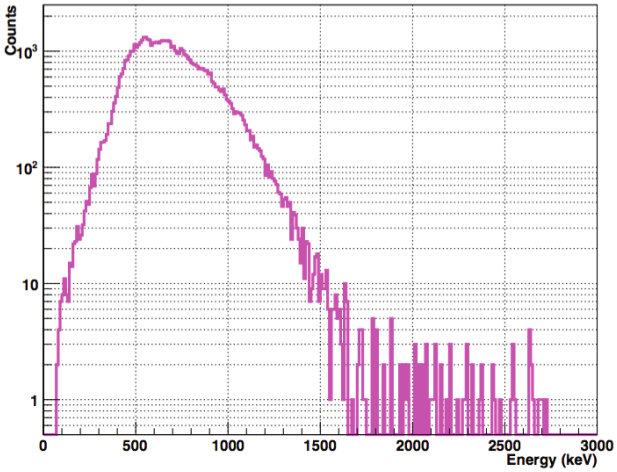

Fig. 6. (Color online) Measured energy spectrum of bremsstrahlung photons for the detector D4 at the view port.

in the bottom side reduces the efficiencies, corresponding to the angular range near 270°.

The measured photon energy spectra were corrected with the simulated efficiencies. Figure 6 shows the bremsstrahlung photon energy spectrum measured using the NaI(Tl) detector (D4) at the view port. The D4 detector was used to monitor a possible variation in ECR plasma intensities throughout the measurements. All the measured spectra in azimuthal angles were normalized to the number of events taken in the same time interval by the D4 detector. While the end-point of the spectrum reaches 1.7 MeV in the radial direction, the end-point energy would be approximately 1.3 MeV if the energy resolution of the NaI(Tl) detector ($\Gamma_\gamma/E_\gamma \approx 7\%$) is taken into account. The maximum kinetic energy ($T_e^{\max}$) that an electron can attain from ECR heating at the cyclotron frequency $\omega = qB/\gamma m_e = qB/E_e$:

$$E_e^{\max} = \frac{qB_{\max}}{2\pi f}, \qquad T_e^{\max} = E_e^{\max} - m_e, \tag{1}$$

where m_e is the mass of an electron, f is the microwave frequency. Here, $E_e^{\max}$ is the total energy of an electron and $B_{\max}$ denotes the maximum magnetic field strength of the ECR ion source. For $f = 28$ GHz and $B_{\max} = 3.6$ T, the maximum kinetic energy is consistent with the observed end-point energy of 1.3 MeV.

The energy spectra for different azimuthal angles were measured using the D1 detector, as shown in Fig. 7. The energy spectrum depends highly on the angles, in particular, yielding a significant difference in the low-energy region. The bump structures appear near 0.3 MeV in some angular positions, which could be due to cumulative Compton backscattering contribution associated with low-energy bremsstrahlung photons. The photon intensity changes drastically according to the azimuthal angles. The slope in the high-energy tail indicates the characteristics of the source of bremsstrahlung photons. The slope of the 210° energy spectrum (overlaid as the

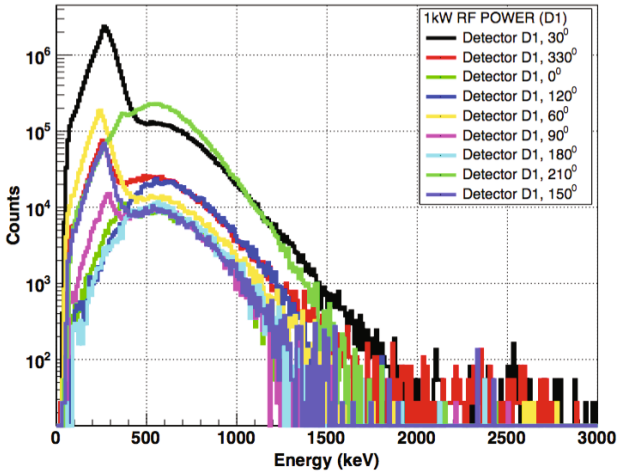

Fig. 7. (Color online) The measured energy spectra in nine azimuthal angles for the detector D1.

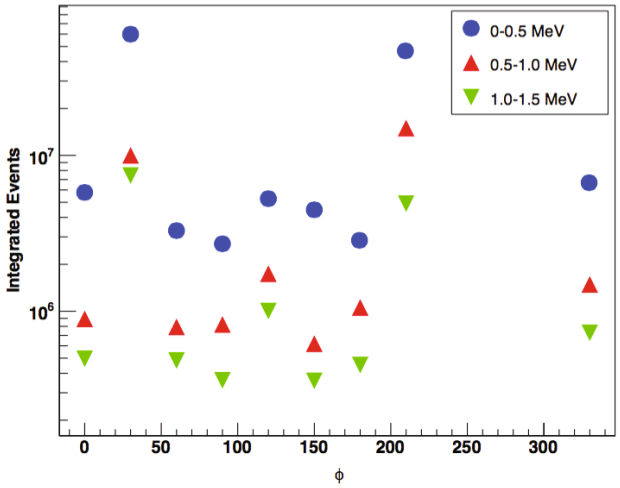

Fig. 8. (Color online) Angular distribution of bremsstrahlung photons in the energy region.

dark green histogram) is different from all others. Moreover, the 30° energy spectrum (overlaid as the black histogram) shows a long tail near 2 MeV, which is beyond the maximum kinetic energy available from ECR heating. The other two detectors show a similar behavior. Therefore, the two different slopes could originate from the different sources of bremsstrahlung photons. It should also be noted that the event rate was as high as several hundreds Hz, bringing a possible pile-up effect with a high-energy tail. However, a full pulse-shape analysis resolved pile-up signals from separate signals so that the pile-up effect could be significantly suppressed.

We integrated photon energy spectra in three energy regions for each azimuthal angle. The angular distributions of the integrated photon yields regarding the three energy regions are shown in Fig. 8. The integrated photon yields are almost two orders of magnitudes different between the maximum and the minimum yields. The two maxima angles are 30° and 210°, which are 180° opposite to each other. It should be noted that the full photo-peak efficiency for 30° is 0.044, while that for 60° is 0.055 in the high-energy region, only 25% difference. However, the integrated yields for the two angles are largely different by more than an order of magnitude. Between the two maximum angles, there seems a local maximum point at 120°. Moreover, the minimum points appear at every 90° angle. The ECR plasma is formed in the shape of a twisted triangular prism, due to the hexapole field. The cross section of the ECR plasma was an inverted triangle in the measurement plane. Electrons at three corners of the triangle are accessible to hit a chamber wall and produce bremsstrahlung photons. The three corners of the plasma triangle correspond to the angles of 30°, 150° and 270°. The last angle position was not accessible due to the support structure. The corner at 30° corresponds to one of the maximum angles, while the second corner at 150° is off the local maximum point at 120°. Furthermore, the maximum point at 210° cannot be explained with the shape of the ECR plasma. It is interesting that the integrated photon yields in the three energy regions are all in phase.

It is highly desirable to measure azimuthal angular distributions for a full dimension of the ECR ion source along the beam axis, to unveil the origin of the high-energy bremsstrahlung photons. The new measurement will help us investigate the contribution from the ECR plasma shape. The modulation phase should rotate by 60° between the inverted triangle at the extraction section and the triangle at the injection section.

III. CONCLUSIONS

We have first measured the azimuthal angular distribution of bremsstrahlung photons from the 28-GHz ECR ion source at Busan Center of Korean Basic Science Institute. The gamma-ray detection system consists of three NaI(Tl) scintillation detectors placed 62 cm radially from the beam axis and a NaI(Tl) scintillation detector at the extraction port for monitoring the photon intensity along the beam axis. The two maxima angles are 30° and 210°, which are 180° opposite to each other. Between the two maximum angles, there seems a local maximum point at 120°. Moreover, the minimum points appear at every 90° angle. The three corners of the inverted plasma triangle correspond to the angles of 30°, 150° and 270°. The corner at 30° corresponds to one of the maximum angles, while the second corner at 150° is from the local maximum point at 120°. Moreover, the maximum point at 210° cannot be explained with the shape of the ECR plasma.

It is highly desirable to measure azimuthal angular distributions for a full dimension of the ECR ion source along the beam axis. The new measurement certainly helps us pin down the contribution from the ECR plasma

by observing the 60° change in the modulation angles between the extraction and the injection sections of the ECR ion source.

ACKNOWLEDGMENTS

The authors would like to gratefully acknowledge support by National Research Foundation of Korea and Korea University.

REFERENCES

[1] R. Geller, *Electron Cyclotron Resonance Ion Sources and ECR Plasmas* (IOP Publishing Ltd, 1996).
[2] D. Hitz *et al.*, Rev. Sci. Instrum. **71**, 839 (2000).
[3] H. Y. Zhao *et al.*, *Proceeding of ECRIS, TUPOT009* (2010).
[4] R. Van der Meer, MSc. Thesis (2008).
[5] H. S. Lee *et al.*, J. Korean Phys. Soc. **55**, 409 (2009).
[6] B. P. Cluggish *et al.*, Phys. Rev. Lett. **81**, 349 (1998).
[7] T. Ropponen *et al.*, Nucl. Instrum. Meth. A **600**, 525 (2009).
[8] L. Schachtera *et al.*, Rev. Sci. Instrum. **75**, 1511 (2004).
[9] D. Leitner *et al.*, Rev. Sci. Instrum. **79**, 033302 (2008).
[10] D. Leitner *et al.*, *Proceeding of the 12th International Conference on Ion Sources* (2007).
[11] T. J. Fessenden, *Technical Report No. 442 MIT-3221-19* (MIT, 1966).
[12] J. Noland *et al.*, Rev. Sci. Instrum. **81**, 02A308 (2010).
[13] J. Y. Park *et al.*, Rev. Sci. Instrum. **87**, 02A717 (2016); J. Y. Park *et al.*, Rev. Sci. Instrum. **85**, 02A928 (2014).
[14] G. F. Knoll, *Radiation Detection and Measurement (3rd Ed.)* (John Wiley & Sons, Inc., 1999).